

# GEOARCHAEOLOGICAL EVIDENCE OF LATE AND POST-ANTIQUITY (5<sup>TH</sup>–9<sup>TH</sup> C. AD) CLIMATE CHANGES RECORDED AT THE ROMAN SITE IN PLEMIĆI BAY (ZADAR REGION, CROATIA)

Fabian Welc

*Institute of Archaeology, Cardinal Stefan Wyszyński University in Warsaw, Wóycickiego 1/3, 01-938 Warsaw, Poland;  
e-mail: f.welc@uksw.edu.pl*

## Abstract

Remains of a vast Roman pottery production complex were found on the shore of the Plemići Bay (Općina Ražanac, Zadar county) in 2012, and confirmed by geophysical survey. Ground-penetrating radar measurements revealed outline of a rectangular building that finds analogies with Roman storehouses (*horreum*). The area occupied by remains of the Roman pottery workshop was covered by immense soil-debris flows. Three geological exposures located to the north of the remains of the Roman building were documented using lithological and malacological analysis, and magnetic susceptibility measurements. The profiles revealed at least three generations of slope sediments, formed in result of intensive soil or debris flows in a dry climate, most probably in 5<sup>th</sup> c. AD. In the next, wet phase sediments were transported downslope and deposited on the Roman structures after 5<sup>th</sup> c. AD. Environmental conditions at Plemići were supply with paleoclimate evidence from the Adriatic region. At ca. 1.5 cal. BP lake levels in the eastern Adriatic area were drastically reduced, probably because of strong decrease in humidity, correlated with the so-called North Atlantic Bond event 3. The drought was followed by a humid episode, also attested at the Plemići archaeological site.

sq

**Key words:** Geoarchaeology, climate change, Roman period, Croatia, Eastern Adriatic

*Manuscript received 19 November 2018, accepted 19 January 2019*

## INTRODUCTION

Remains of a large Roman pottery and ceramics production complex were found on the shore of the Plemići Bay (Općina Ražanac, Zadar county) in 2012 (Fig. 1) (Lipovac Vrkljan, Konestra, 2018). Numerous fragments of Roman vessels, roof tiles and elements of infrastructure, such as channels and walls, were found in the earth profiles, which can be mostly dated to the first centuries AD. Underwater archaeological research carried out in the bay proved that in Roman times a harbor was established there, most probably connected with the ceramic workshop (Ilkić and Parica, 2017; Parica and Ilkić, 2018).

Within the Project RED (*Roman Economy in Dalmatia*, HRZZ, IP-11-2013-3973), a field survey and geophysical prospection have been carried out in 2018 at the Plemići Bay. One of the goal of the survey was to review the possible extension of the Roman workshop and establish its chronology (Ilkić and Parica, 2017; Lipovac Vrkljan *et al.*, 2017; Welc, 2018). The survey was supplemented with geoarchaeological analysis of sediments exposed in sections

located to the west of the ancient Roman building remains, in order to reconstruct environmental conditions during its occupation phase and in later times.

## LOCAL GEOLOGICAL SETTINGS

Plemići Bay is located within the frame of the Radovin syncline composed mostly of Middle Eocene clastic sediments, also referred to as flysch, which are underlain by Cretaceous and Palaeogene limestones (Schubert, 1903, 1905; Schubert and Waagen, 1913; Majcen and Korolija, 1970; Babić and Zupanić, 1998). Sandstones dominating in Plemići Bay area are fine to coarse-grained, with a characteristic grey colour. They contain 45% to 60% carbonate particles and limestone clasts. Conglomerates occurring in the same region consist mostly of limestones, sandstones and chert clasts within a sand matrix. In the coarser-grained conglomerates, *nummulites* are common in the sandy matrix (Babić and Zupanić, 1998). In the study area residual soils that originated from weathered

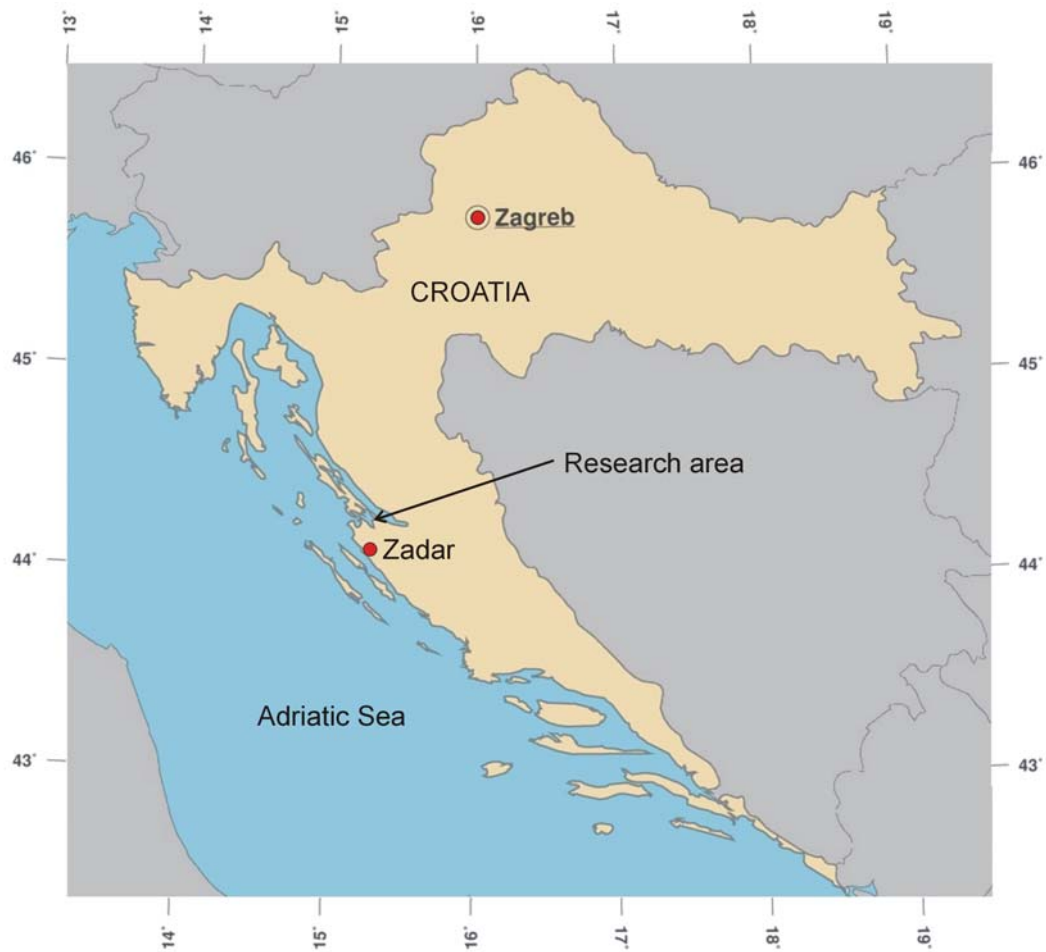
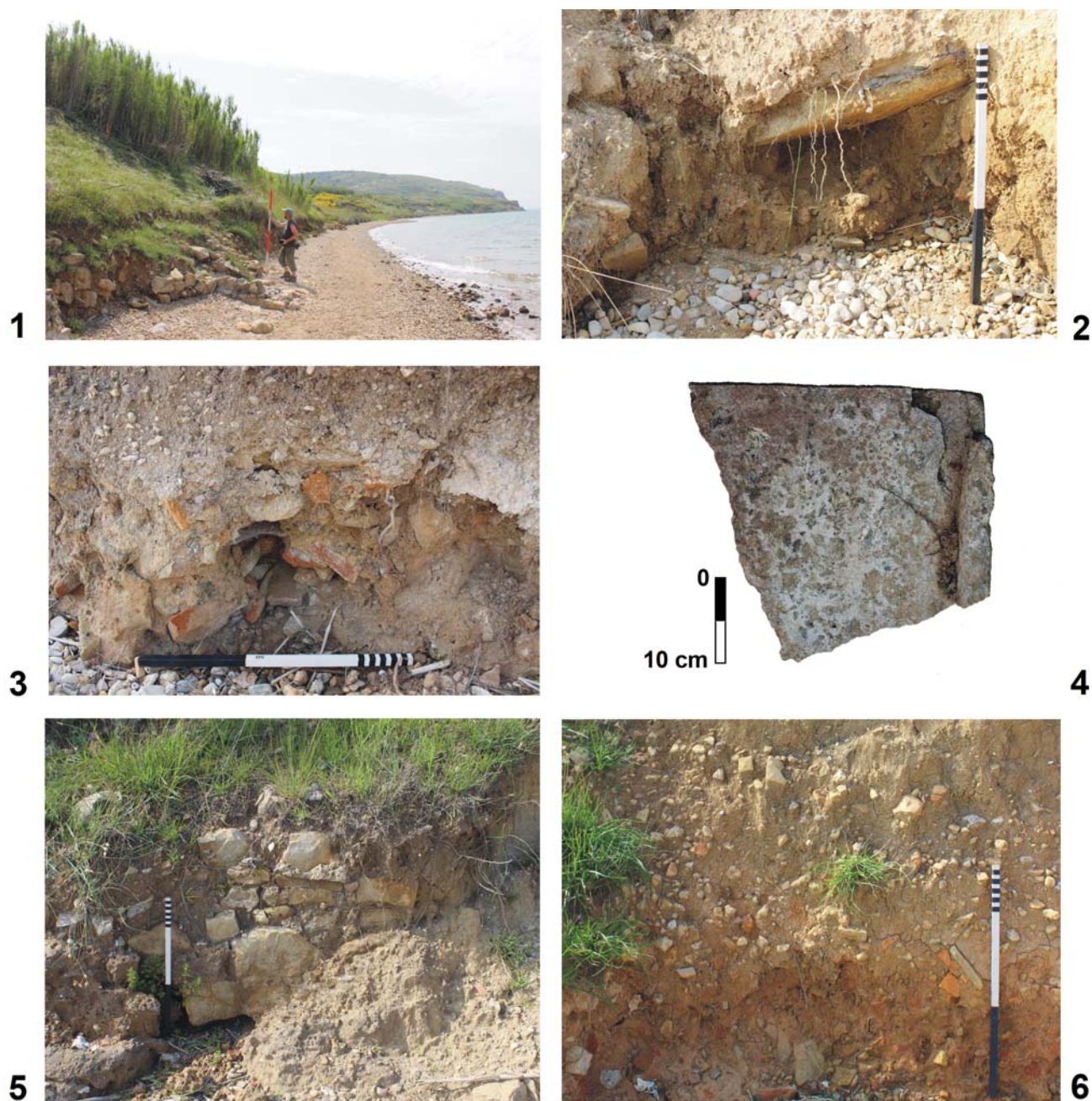


Fig. 1. Map of Croatia with the location of Plemići Bay (above) and photograph of the bay (below) taken from the south (Photo F. Welc).

flysch deposits dominate. They have an important hydrogeological function forming an impermeable barrier for the infiltration of the karst groundwater (Fritz and Pavičić, 1991).

The geoarchaeological survey area is located in the southern part of Plemići Bay. Nowadays from the west the site is cut by an erosional, NE–SW-oriented valley filled with thick Quaternary sediments, which were deposited



**Fig. 2.** In all natural exposures located on the seacoast at Plemići Bay, deposits of both natural and anthropogenic origin are strongly disturbed, as evidenced by numerous archaeological finds and other traces of past human activity. 1 – Remains of a Roman structures covered by slope sediments. 2, 3 and 4 – Roman ceramic tiles visible in exposures at the beach. 5 – Remains of a stone wall visible in an exposure on the coast. 6 – Numerous Roman pottery fragments visible in a natural profile (slope deposits) (Photo F. Welc).

directly on the top of Middle Eocene clastic series (flysch). In part of the coast, the subsurface layers, both of natural and anthropogenic origin, are strongly disturbed, as evidenced by numerous fragments of ceramics and other traces of past human activity visible in natural exposures, however almost always in secondary contexts (redeposited). This material can be dated to the Roman period and mostly seems to be moved and intermingled from the higher ground, which suggests very intensive earth movement processes in the past. In effect, silty sand was

deposited above the archaeological site, creating a slope inclined at 35–40° (Fig. 2).

In 2018, the area located in close vicinity to the remains of the Roman stone construction was surveyed using ground penetrating radar (GPR). The directors of the field archaeological investigations were Drs Ana Konestra and Goranka Lipovac Vrkljan (Institute of Archaeology, Zagreb, Croatia). The geophysical and geoarchaeological survey was headed by Dr hab. Fabian Welc (Institute of Archaeology, Cardinal Stefan Wyszyński University in Warsaw, Poland).

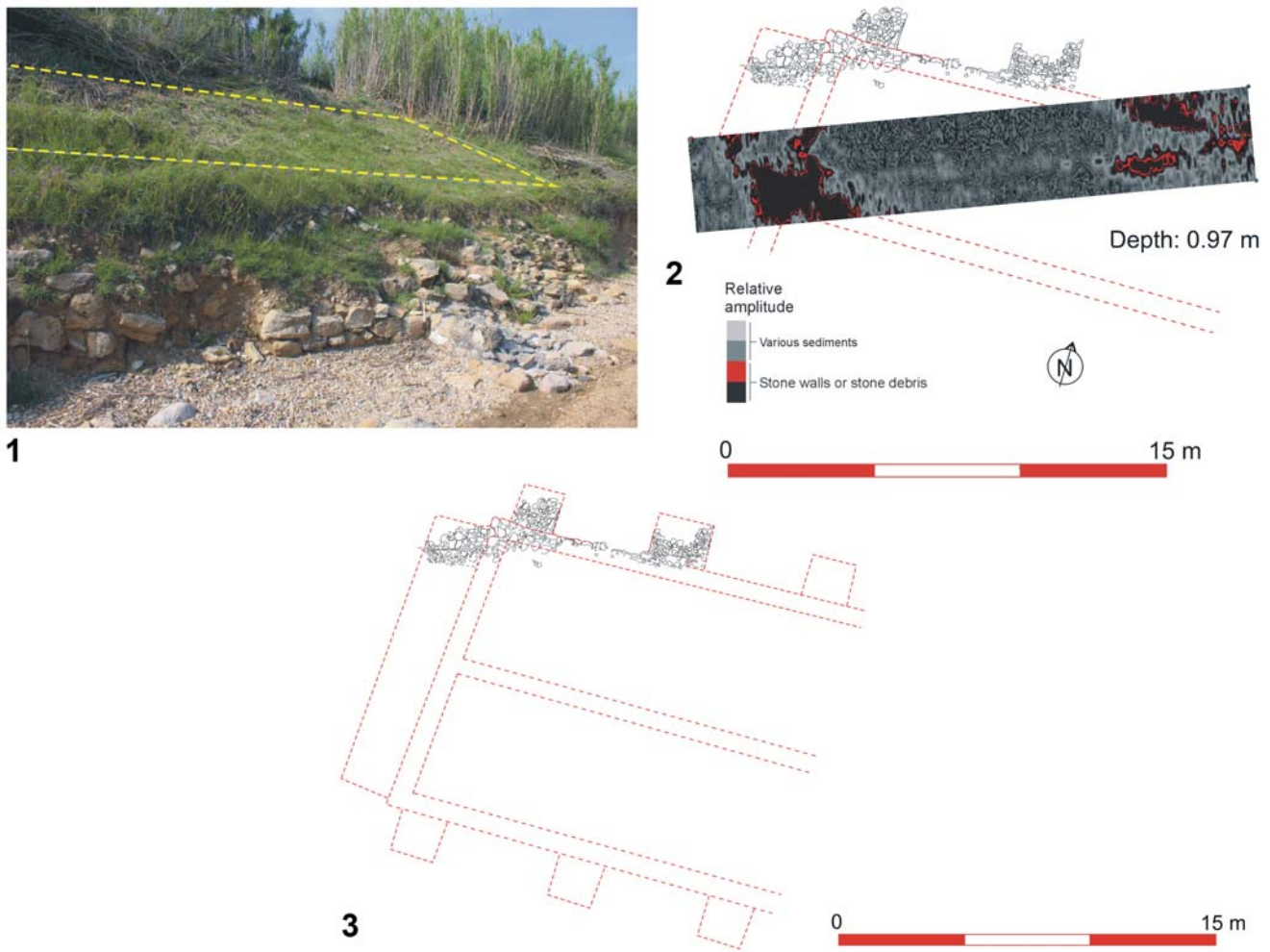


**Fig. 3.** Results of geophysical survey in Plemići Bay with the use of a ground – penetrating radar. 1 – GPR profiling at Plemići Bay was performed within the narrow and long, W–E-oriented polygon, which is directly adjacent to the seacoast and to the zone occupied today by the stone remains of the Roman building. 2 – GPR slices revealed the outline of a rectangular structure with a length of over 15 m and a width of about 5 m. The western wall of the building continues its course towards the south, which indicates that the structure is significantly larger and occupies a much larger area. 3 – The reconstructed plan of the building, based on geophysical data, presents a structure that finds analogies with Roman storehouses – *horreum* (Photographs, processing and drawing: F. Welc).

## METHODS

### Ground – penetrating radar

The GPR is a mobile and highly effective method of shallow sub-surface geophysical prospection, based on emitting electromagnetic waves with frequencies in the range of high and ultra-high frequency and registration of the impulses reflected from buried archaeological features (for the application of the GPR method in archaeological surveys see e.g., Conyers and Leckebusch, 2010; Conyers, 2013, 2016a, 2016, 2018; Welc *et al.*, 2016, 2017a, 2017). The Mala/ABEM radar system, produced by the Swedish company Mala Geosciences was used during the survey. The prospection was carried out with the application of a screened transmitting antenna, with a nominal frequency of the emitted EM waves at 450 MHz. During prospecting, the profiles were separated from each other at 0.5 m. Because

dry sands with a clay admixture prevail in the study area, the average velocity of the electromagnetic wave propagation was accepted at the level of 0.07 m/ns.

### Sedimentological analysis

Three geological exposures located directly to the west of the Roman structures have been documented in order to reconstruct the sedimentary environment and indirectly also the climatic conditions during the deposition of the sediments. All profiles were macroscopically studied, documented and sampled at intervals of 5 cm. The collected samples were selected for further laboratory research such as grain size analysis and malacological studies. Supplementary, magnetic susceptibility measurements were also performed in the field, directly on the surfaces of the exposures (at intervals of 5 cm).

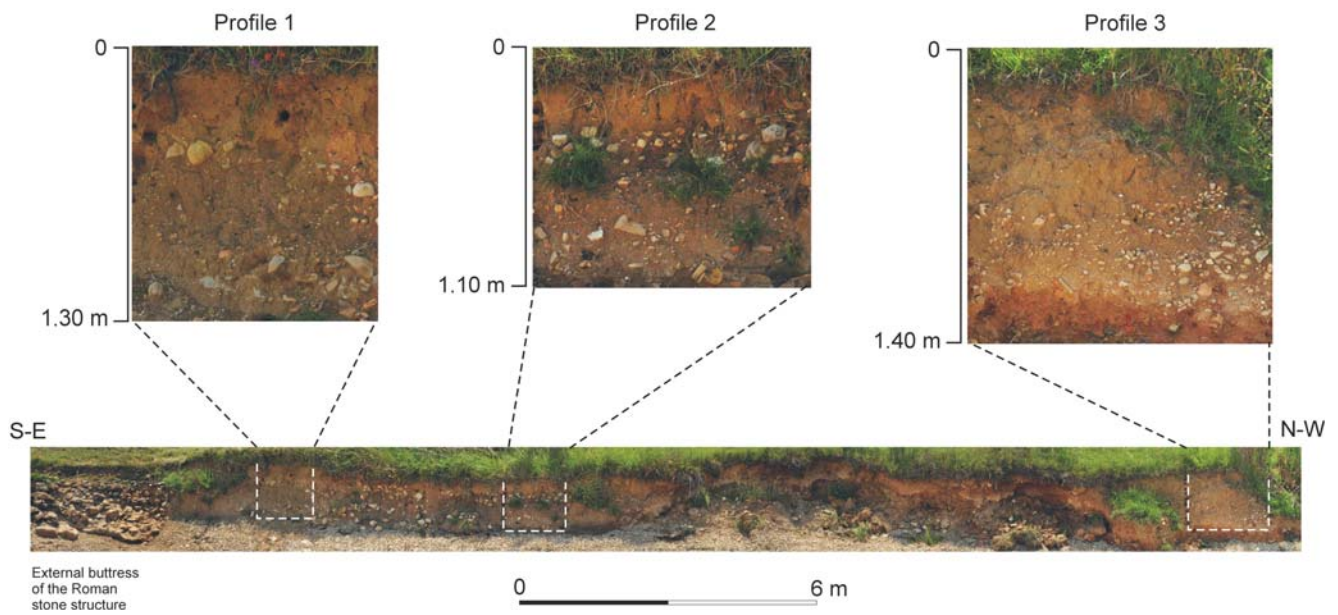


Fig. 4. Location of the three exposures documented to the west of the Roman structures (Photo: F. Welc).

Grain size analysis of the samples collected in profile 1 was performed by Dr J. Trzciński and Msc M. Zaremba (Institute of Archaeology Cardinal Stefan Wyszyński University in Warsaw). The samples from the layers 2 (depth 0.25 m), 3 (depth 0.45 m), 4a (upper part) (depth 0.65 m), 4b (lower part) (depth 1.00 m), 5 (depth 1.20 m) and 6 (depth 1.35 m) were selected to perform granulometric analysis (Fig. 4). Due to the fact that the sediments are dominated by a silt-clay fraction (diameters of the mineral particles are  $<0.05$  m), the aerometric (sedimentary) method was applied, which fractionates the sediment samples from a suspension. The measurement is based on Stoke's law, according to which the flow velocity of a spherical object is directly proportional to its diameter and density. It also depends on standard gravity, specific density and water viscosity. Grain size analysis was conducted according to the norm (PN-88/B-04481). Fractions  $>0.05$  mm were selected for sieve analysis, whereas fractions  $<0.05$  mm were

subjected to sedimentation analysis (for methodology see also Trzciński *et al.*, 2016).

#### Malacological studies

The malacofaunal analysis was performed by Dr Marcin Szymanek (Faculty of Geology, University of Warsaw). Malacological studies included 7 selected samples taken from all 3 profiles (Fig. 5). The identification of the malacological material was carried out under a stereoscopic microscope (up to  $64\times$  magnification) with the use of keys and atlases for the determination of malacofaunal genera (Welter-Schultes, 2012). Due to the low individual abundance, a qualitative analysis was performed, however it was impossible to apply extensive quantitative methods proposed by Ložek (1964) and Alexandrowicz and Alexandrowicz (2011).

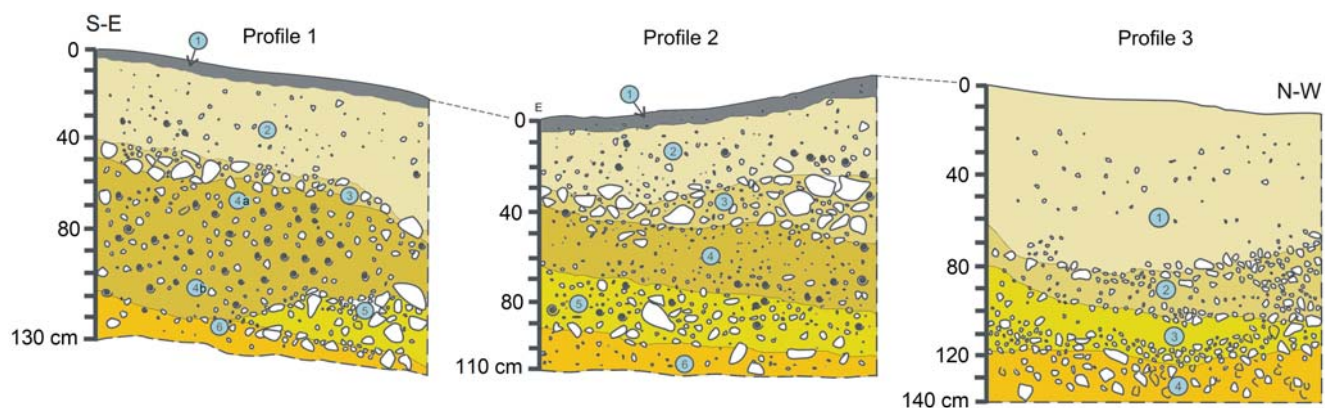


Fig. 5. Drawing documentation of the three geological profiles exposed to the west of the Roman stone structures. Individual layers distinguished in the profiles are marked with a numbers in circles (Drawing: F. Welc).

### Magnetic susceptibility (MS) measurements

Measurements of magnetic susceptibility (MS) of the sediment samples were performed with the use of an SM30 kappameter produced by ZH Instruments, at point reading of the MS value in an interval of 5 cm along the entire profile length (Fig. 5). The producer determines the device resolution at  $1 \times 10^{-7}$  MS units in the SI system (www.zhinstruments.com). Generally speaking, magnetic susceptibility measurements allow determining a degree of “magnetisation” of the studied sediments (Dearing, 1994). The most important factor affecting the value of magnetic susceptibility is the lithological composition and grain size characteristics of the sediment (Sandgren and Snowball, 2001). Increased content of ferromagnetic minerals, such as magnetite or hematite, generates a higher MS value, whereas biotite, pyrite, carbonates and organics influence their reduction (Dearing, 1994).

## RESULTS

GPR profiling was performed within a narrow and long, W–E-oriented polygon, directly adjacent to the sea coast and to the zone occupied by the stone remains of the Roman construction (Fig. 3: 1). As mentioned above, the Roman structures detected at Plemići Bay were covered by soil and debris deposits which strongly attenuate electromagnetic waves. In effect, the depth range of GPR prospecting did not exceed 2 m. At 0.6–0.7 m depth, the time slices (GPR maps) revealed two parallel walls and one additional wall, oriented perpendicularly to the two previous ones, at the depth between 0.70 and 1.0 m (Fig. 3: 2). When the GPR

time slices prepared for individual depth levels are combined with the plan of the visible architecture on the seashore, not only the original outline of the building can be reconstructed but also its function can be considered (Fig. 3: 3). The remains of the walls preserved on the seacoast indicate a typical Roman building technique (*opus incertum*) with wall faces and internal cores both built from irregular limestone and sandstone blocks bounded with lime and sand mortar (Cech, 2017). Only the external faces of the walls were raised from partially well dressed and more or less uniform stones.

The plan of the structure preserved on the seacoast combined with selected GPR slices revealed the outline of a rectangular building with a length of over 15 m and a width of about 5 m (Fig. 3: 3). GPR plans clearly show that the western wall of the building continues its course towards the south, which indicates that the structure was significantly larger and occupies a much larger area. It seems that the southern wall of the building captured in the GPR images is in fact the internal wall, which most likely divided the building into two separate parts. If this interpretation is correct, the building was >15 m long and >12 m wide. A reconstruction based on geophysical data revealed a structure that may find analogies with typical Roman warehouses (*horreum*) (Fig. 3: 3). Usually these magazines were built with ramps rather than staircases to provide easy access to the upper floors (Rickman, 1971; Dominguez, 2011). The lowermost section (or perhaps foundations) of the northern wall of the building is poorly preserved but is still visible in the profile on the beach. On the other hand, taking into account the results of the geophysical survey, it can be assumed that the western wall and part of the inner dividing wall have been preserved to a height of at least 3 m.

Table 1. Admixtures in the profiles 2–6.

Grain diameter [mm]	Sample symbol					
	2	3	4a	4b	5	6
>5	– grains cemented with CaCO <sub>3</sub> – ceramic fragments – root fragments	–	– grains cemented with CaCO <sub>3</sub> – whole shells – ceramic fragments	– grains cemented with CaCO <sub>3</sub> – whole gastropod shells	– ceramic fragments – limestone fragments	–
2–5	–	–	–	– ceramic fragments – root fragments	– whole gastropod shells – ceramic fragments – organic matter	– root fragments – crushed shells
1–2	– whole and crushed shells	– whole and crushed shells – rounded grains	– crushed shells	– root fragments – crushed shells – rounded grains	– crushed shells	– crushed shells
0.5–1	– crushed shells – dark minerals – sharp-edged grains	– dark minerals – rounded grains	– crushed shells – organic matter – sharp-edged grains	– dark minerals – rounded grains	– dark minerals – crushed shells	– crushed shells – dark minerals – sharp-edged grains
0.25–0.5	– crushed shells – dark minerals – organic matter	– organic matter	– crushed shells – dark minerals – organic matter – sharp-edged shells	– dark minerals – organic matter	– dark minerals – organic matter	– crushed shells – sharp-edged grains
0.1–0.25	– dark minerals – organic matter – rounded grains	– organic matter	– dark minerals – organic matter	– organic matter	– organic matter	– crushed shells – dark minerals – sharp-edged grains
0.05–0.25	– dark minerals – organic matter	– organic matter	– dark minerals – organic matter	– rounded grains	– rounded grains	– dark minerals

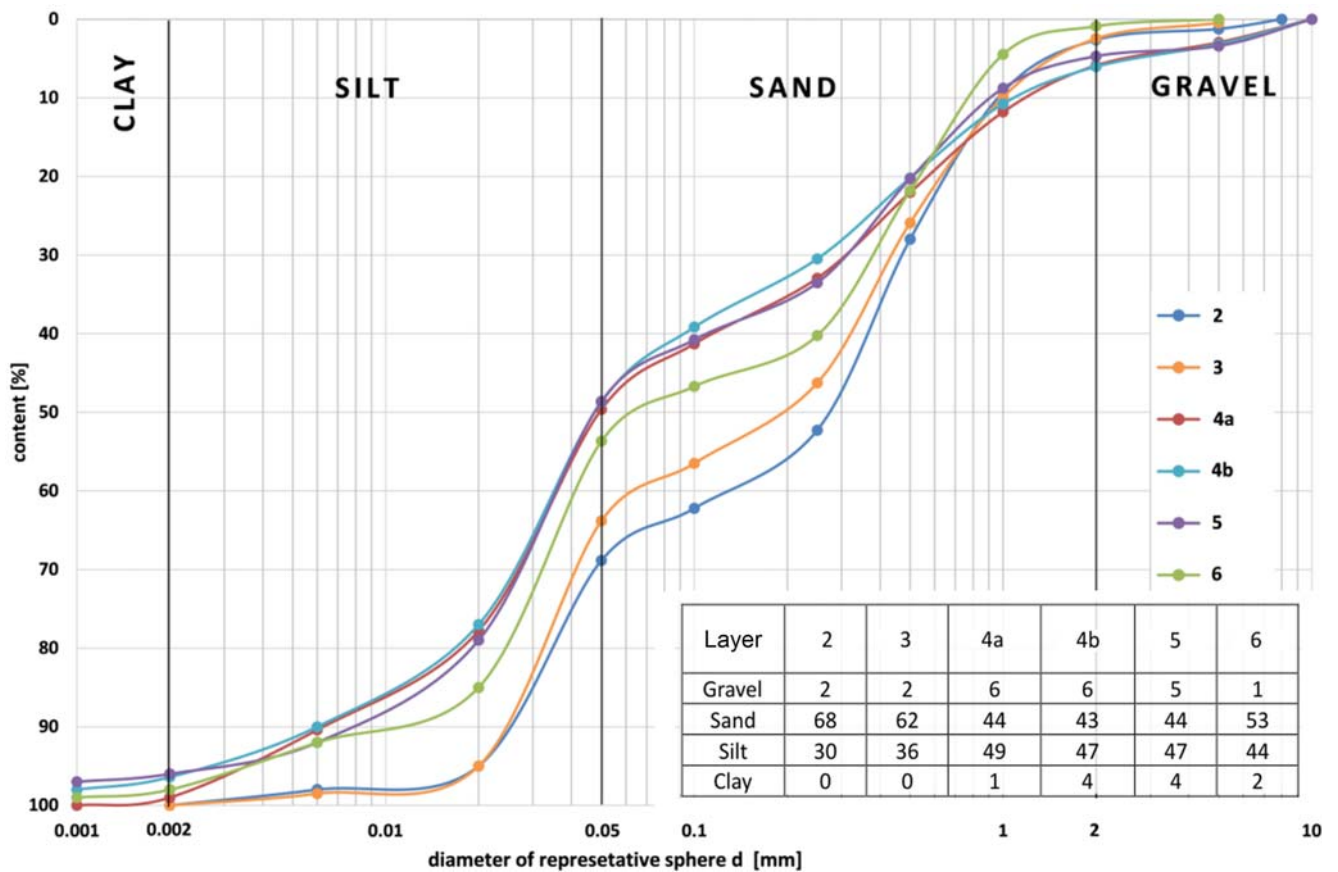


Fig. 6. Graphs presenting the results of granulometry analysis performed for profile no. 1 (Drawing: J. Trzciński, M. Zaremba).

### Paleoenvironmental studies

Three geological exposures located to the west of the Roman stone structures revealed at least three generations of slope deposits, which mainly consist of silty sand, brown in colour (Figs. 4 and 5). They are massive, unstructured, but show graded bedding towards the top. A characteristic feature of these sediments is high mixing and sharp transitions (boundaries) between the coarse and fine-grained material.

Results of grain size analysis performed for profile 1 are illustrated on the grain size curves (Fig. 6). The layers distinguished in the profile distinctly differ in the content of particular fractions (clay, silt, sand and gravel). In the analysed sequence sand and silt fractions prevail, whereas gravel and clay fractions are subordinate. The largest variability occurs in the sand fraction, dominating in the upper and lower part of the profile, and with minimum contribution in the middle part. Lower variability was observed in the case of silt fraction, whose contribution increases in the middle and lower part of the profile. The largest content of gravel and clay fractions is observed in the middle part of the succession.

In all parts of profile 1 there are small fragments of

plant roots, particularly in the upper layers and in coarser fractions, and poorly decomposed organic matter, whose contribution increases in the upper beds (Table 1). In fractions  $>2$  mm there are commonly small fragments of Roman pottery and finer grains strongly cemented with calcium carbonate. In fractions  $<1$  mm there are dark minerals, whose content increases in successively finer fractions. Medium-grained fractions are dominated by sharp-edged grains, rounded grains being subordinate.

All analysed exposures reveal higher values of magnetic susceptibility in the lower parts, i.e. between  $0.1$  and  $0.8 \times 10^{-7}$  MS units (Fig. 7). In the upper parts of the profiles, these values are significantly smaller (Fig. 7).

In the three described profiles, several species of molluscs have been identified, represented by a total of 110 specimens. The number of species in the tested samples varies from 1 to 6, recorded in profile 2, respectively in layers 4 and 2 (Szymanek, 2018). The number of specimens varies from 4 (profile 1, layer 2) to 29 (profile 1, layer 4) (see Fig. 5). The assemblage of the identified species is consistent in relation to the environmental requirements of the recorded fauna (the only exception is profile 3, layer 2, where land snails co-occur with two marine species – the snail *Cerithium vulgatum* and the

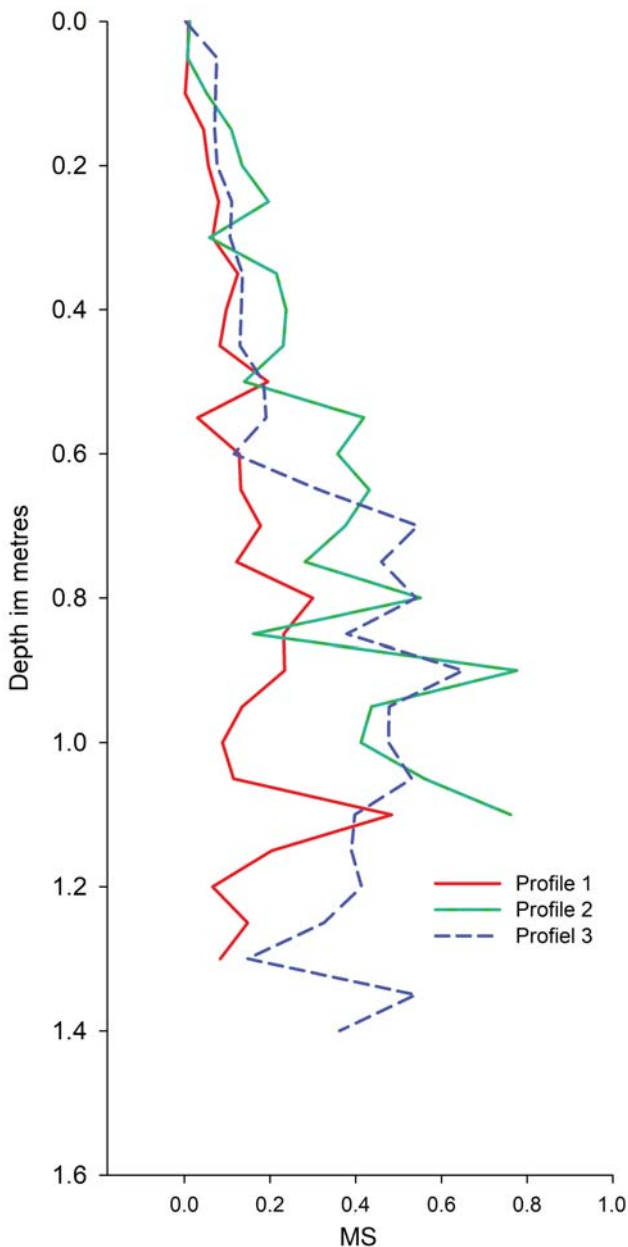


Fig. 7. Graphs presenting the results of magnetic susceptibility measurements for the profiles no. 1–3 (Drawing: F. Welc).

bivalve *Donacilla cornea*. Both species inhabit the sandy bottom in the inter-tidal coastal zone and are a common fauna of the Mediterranean region (Samek, 2004; Petović *et al.*, 2017).

#### Paleoenvironmental interpretation

Large variability and presence of all main fractions in layers distinguished in a relatively thin succession of profile 1 indicate very short transport of the material. This assumption is confirmed by the location and morphology of the analysed strata. Their almost horizontal position in

a terminal zone of the slope succession points out to a wide and almost uniform distribution of material flowing from a higher land area. Furthermore, the entire succession revealed a large content of organic remains (see Table 1). These include whole gastropod shells occurring in coarser fractions >2 mm as well as their crushed fragments, commonly occurring in successively larger amounts in the finer fractions. The documented lithological and sedimentological features of profile 1 confirm short but dynamic sediment transport and its local provenance. Gastropod shells were crushed during movement of sediment down a slope. Large contribution of such fragments indicates intense flow episodes, in effect of which subsequent beds were formed. Relatively low content of plant root fragments may suggest that periods of plant vegetation were interrupted by down slope flows. Short transport and high energy of the slope episodes are confirmed also by high contents of dark minerals in the analysed layers and by a large content of sharp-edged quartz grains (Table 1).

All documented sedimentary series seem to have resulted from massive soil or debris flows. The latter are commonly caused by intensive surface water flow, due to heavy precipitation, that erodes and mobilizes loose soil or rock on the slopes. In other words, debris flows occur when a viscous combination of sediment saturated with water moves and is transported downward. What is important is that debris flows are typically deposited as clasts or mud-rich levees that give way to lobes down-fan as energy decreases. Fine grained lobes usually dominate on low-angle fans. It is assumed that alluvial fan sedimentation depends on climatic and tectonic conditions. Aggradation will occur when water saturated with sediment is transported down-fan (typically wet conditions), whereas dissection occurs when fluids are sediment starved (dry conditions). Thus, alluvial fans have proven to be useful indicators of past climate (Hooke, 1967; Harvey, 2002; Doom, 2009). Most authors speculate that fan aggradation occurs during moist periods due to greater sediment production, whereas fan erosion occurs during arid periods (Doom, 2009). It is argued that fan erosion occurs due to fluids exiting the catchment area without sediment. Decreased vegetation during arid periods will result in lower slope stability and increased incision (Doom, 2009).

There is no doubt that the current topography of the Plemići Bay had much changed since ancient times as a result of intensive erosion. Low terraces surrounding the erosional valleys were created in the past as a result of slope processes (Fig. 8). In effect, all ancient Roman structures located near the seashore, such as workshops and other buildings, were covered by mass movements of sediments. A characteristic feature of the geological structure of Plemići Bay area are thick packages of Quaternary deposits (sand and sandy silt, clay) that have been deposited directly on the top of Eocene clastic series. The contact between the two formations created a kind of slip surface that facilitated the formation of debris flows. Archaeological material is in most cases is displaced and intermingled, suggesting that slope activity has been initiated already in a distant past,



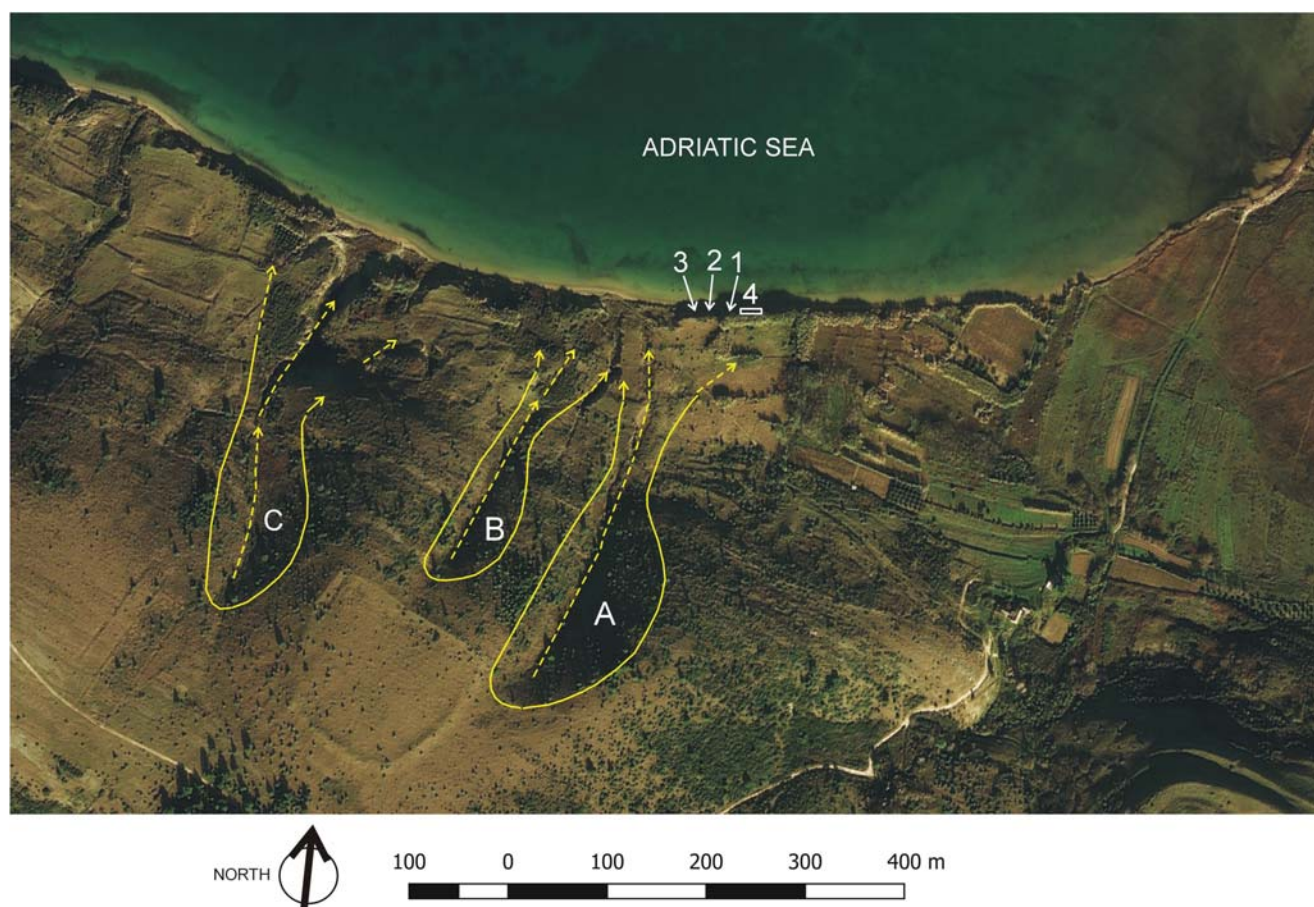


**Fig. 8.** Location of the studied geological profiles (1–3) near the remains of the Roman structures (4), which was surveyed with the use of the GPR method. Extensive erosional niches and valleys, being the remnants of slope processes, are visible above the Roman archaeological site (A–C).

most probably in a post-late Antiquity period. Most likely the main triggering mechanism for these processes were periodical and simultaneously intensive rainfalls, which initiated surface transport of the sediments by periodic runoff *via* the erosional valleys, whereby small alluvial fans were created at the valley outlet.

The assumptions presented above seem to be confirmed by results of magnetic susceptibility measurements (Fig. 7). It is assumed that the magnetic properties of sediments reflect climate change (Bloemdal and deMenocal, 1989; Snowball, 1993; Peck *et al.*, 1994). Ferromagnetic minerals are delivered to the sediments mainly due to surface runoff or along with river water. Intensification of erosion by periodic rainfalls causes more intensive supply of ferromagnetic material to the soil, which directly affects higher MS values. The distance of allochthonous material transport is also important in this case. A higher value of magnetic susceptibility in the sediments is also often a derivative of the degree of erosion, which is intensified in dry periods. During stable humid intervals, due to the development of a vegetation cover, the volume of ferromagnetic minerals is significantly reduced (Snowball, 1993). All examined exposures in Plemići Bay reveal in the lower parts much higher magnetic suscepti-

bility, which suggests that these sediments were formed under relatively dry climate conditions. Slope sediments documented in the lower parts of the examined profiles seems to have been transported downslope during a wet interval which was preceded by a dry period when the plant cover was significantly reduced and extensive erosion processes dominated. Relevant data confirming this assumption was also provided by the malacological analysis. The shell material from the Plemići site undoubtedly indicates land origin of the sediment in which it was found. The composition of the mollusc assemblage in the remaining profiles indicates development of the fauna in an open landscape. Ten species are land snails, typical of open and warm environments. They live in dry and warm grassy meadows, sunlit slopes and can also appear in zones of rock erosion, buried up to 10 cm in the ground (e.g. *Pomatias elegans*, *Chondrula tridens*, *Rumina decollata*, *Helix cincta*; Welter-Schultes, 2012). Three species, *P. elegans*, *Granaria frumentum* and *Imparietula seductilis*, are closely related to the carbonate rock substrate, and the group is dominated by *P. elegans*, a typical species of coastal grassy meadows, open forests, shrubs, with a layer of rubble facilitating inward penetration (Welter-Schultes, 2012; Szymanek, 2018).

## Discussion

Environmental conditions documented within the slope sediments at the Roman site in Plemići Bay find indirect evidence in the paleoclimatic studies from the Mediterranean region, pointing out to significant differences between eastern and western basins (Kuzucuoğlu *et al.*, 2011; Peyron *et al.*, 2011; Giraudi *et al.*, 2011; Zanchetta *et al.*, 2011). In this context, the Holocene climate reconstructions from Croatia may provide a link between the two sub-basins (Rudzka *et al.*, 2012). The most important palaeoclimatic data is supplied by the study of bottom deposits from the Blue Lake (Modro Jezero) near Imotski in Croatia. According to Miko *et al.*, (2015), this lake records reflect variation between low stands (droughts) and high water levels during the late Holocene. The obtained 8 m-long sediment core can be dated back to 2.4 ka BP. The following laboratory methods were applied during the study of this core: advanced colour analysis of the sediment (identifying colour differences using L\*a\*b\* coordinates), magnetic susceptibility (MS) measurements, dating using the AMS <sup>14</sup>C method, micro-physiography, grain size analysis, and determination of the nitrogen and organic carbon content. The L\*parameter (lightness value) is connected with the organic carbon content to detect drought episodes (Miko *et al.*, 2015) (Fig. 9). Based on the combination of these parameters with discontinuities detected in the sedimentation rate, it was possible to reconstruct environmental changes in the Blue Lake during the last 2400 years. In 1.6–1.3 cal. ka BP, the lake was characterised by intensive carbonate sedimentation, which may be correlated with frequent drought periods. After that, ca. 1.3 ka cal. BP, the lake became much deeper with no visible breaks of the sedimentation rate, mostly due to higher rate of water discharge (Miko *et al.*, 2015). The next important core in the context of this study was obtained from the biggest Croatian – Vrana Lake on the island of Cres (Ilijanić and Miko, 2016) (Fig. 9).

Based on the paleoenvironmental reconstruction of Lake Vrana development, in the 1.5–1.2 cal. ka BP, the L\* parameter notes a significant fall correlated with the decrease of silt content in the sediment and subsequent percentage increase of the clay fraction, Al, Ca content and decrease of the Sr/Ca ratio and TOC content. These data indicate fall of the lake water level (drought) accompanied by precipitation of Ca in the sediment and smaller supply of terrigenous material to the basin (lack of rainfall). At the end of the discussed period, ca. 1.3 ka BP, all these parameters note opposite trends, which indicates renewed deepening of the basin and increased supply of terrigenous material (higher contents of Al and the silt fraction), probably due to increase rainfall in the vicinity of the lake (Fig. 10).

Important data were supplied also by palynological studies of bottom sediments from the Lake Shkodra in Albania (Sadori *et al.*, 2015) (Fig. 9). Three parallel cores were drilled in this lake, with overlapping sediment record cored down to 7.26 m depth (Van Welden *et al.*, 2008). The obtained data clearly indicates that at ca. 1.5 cal. ka BP the forest around the lake was drastically reduced, probably

due to strong decrease in humidity. According to Sadori *et al.* (2015) this episode shows a strict coincidence with the so-called North Atlantic Bond event 3 (see Bond *et al.*, 1997). This dry interval was followed by a humid episode, the beginning of which can be dated at ca. 1.4 cal. ka BP (Zanchetta *et al.*, 2012). Comparable results have been supplied by studies of a stalagmite from Ceremosnja Cave (eastern Serbia), dated back to 2.3 cal. ka BP (Fig. 9). Its paleoclimate record based on stable isotope data indicates a warm period between ca. 1.5–1.2 cal ka BP, terminating with a colder phase which can be dated at ca. 1.1 ka BP (Kacanski *et al.*, 2001). Similar results were brought by studies of two speleothems MOD-21 and MOD-22 from the Modrič Cave (Croatia) (Rudzka *et al.*, 2012) (Fig. 9). Drier conditions, were recognised by a gradual narrowing of the MOD-22 stalagmite (higher  $\delta^{13}\text{C}$  value), can be dated to 1.5–1.3 cal. ka BP. According to Rudzka *et al.* (2012) this dry episode appears to correspond to the transition from the Migration Period to the Middle Ages (Fig. 9).

A significant supplementation of the above presented compilation of paleoclimatic data are results of dendrochronological studies based on 7284 precipitation sensitive oak ring width series, mostly from northern Europe (Germany and France) (Büntgen *et al.*, 2011) (Figs. 11 and 12). To understand the interannual to multicentennial climate fluctuations in Europe – the AMJ (April-to-June) precipitation index was used. The obtained results show a low precipitation index from 1.5–1.4 cal. ka BP. The AMJ precipitation and the JJA (June-to-August) temperature began to increase gradually from ca. 1.3 cal. ka BP and reached climate conditions comparable to those of the Roman period ca. 1.2 cal. ka BP. According to Piva *et al.* (2008) and Rogerson *et al.* (2011) warmer and drier conditions during the transition from the Migration Period to the Medieval epoch dominated in the entire Adriatic region and also in adjacent areas. For example, the population in the eastern Mediterranean region continued to grow until ca. 1.4 cal. ka BP, when a shift in climate appears to have been contributed to the widespread changes occurring in social processing and population rates, but also changes in the settlement pattern (Bookman *et al.*, 2004; Jones *et al.*, 2006; McCormick *et al.*, 2012).

It is obvious that the dry period and the succeeding humid interval recorded in the slope sediments from the Roman archaeological site in Plemići Bay should be discussed in a wider, transregional context. The record of climate changes taking place at the end of the Roman Empire and after its fall (5–9 century AD) is presently very incomplete and obviously very complex. Today, climatic conditions in the Mediterranean region are dominated by a seesaw in precipitation anomalies between its south-eastern and western basins (Dunkeloh and Jacobeit, 2003). This seesaw in climatic diversity is correlated with changes of the sea level pressure (SLP) and variability over the North Atlantic region, ceased mostly by the North Atlantic Oscillation (NAO) (Dermody *et al.*, 2012). In turn, the NAO index is proposed to have oscillated with a periodicity of 1.5 kyr known as the Holocene Bond climatic events (see Bond *et al.*, 1997, 2001). During

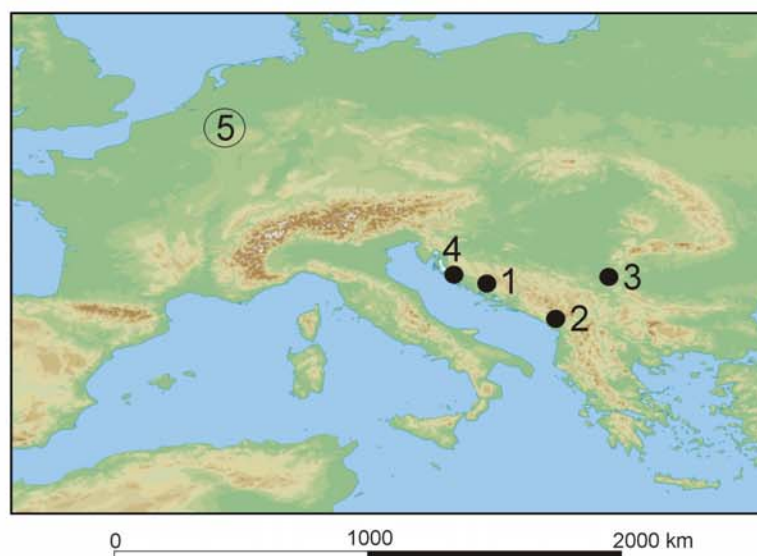
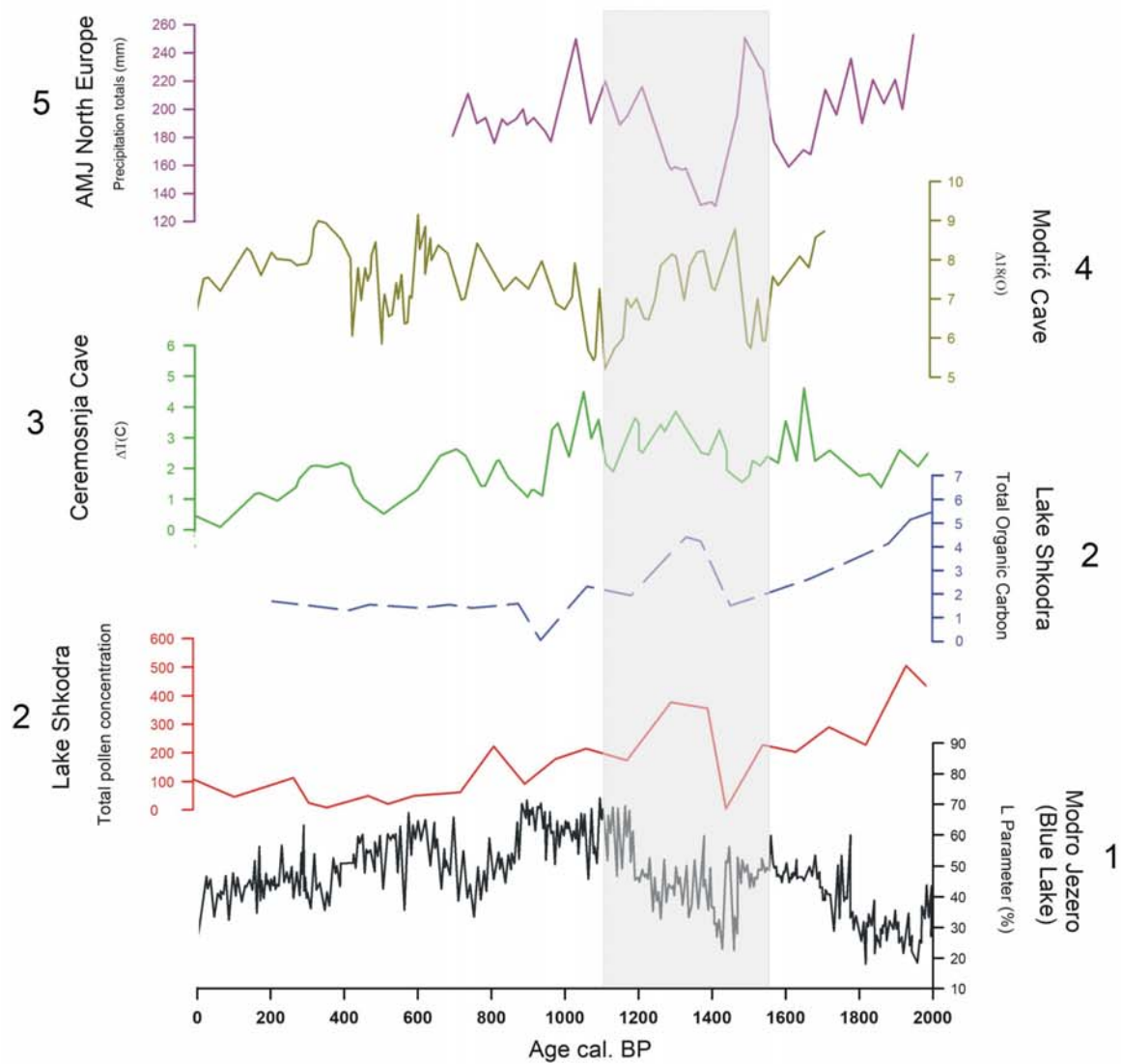


**Fig. 9.** Comparison of normalized composite proxy records from the eastern Adriatic region and north Europe. 1. Blue Lake (Modro Jezero): distribution of the L\*parameter (After: Miko *et al.*, 2015). 2. Core SK-13 from Lake Shkodra: total pollen concentration (After: Sadori *et al.*, 2015). 3. Ceremosnja Cave: reconstruction of the average temperature based on isotope studies of the stalagmites (After: Kacanski *et al.*, 2001). 4. Modrić Cave: interpretation of the stable isotope record based on studies of stalagmite MOD-22 (a) (After: Rudzka *et al.*, 2012). 5. Reconstructed AMJ precipitation based on 7284 precipitation-sensitive oak ring width series mostly from Northern Europe (Germany and France) (After Büntgen *et al.*, 2011). (Drawing: F. Welc).

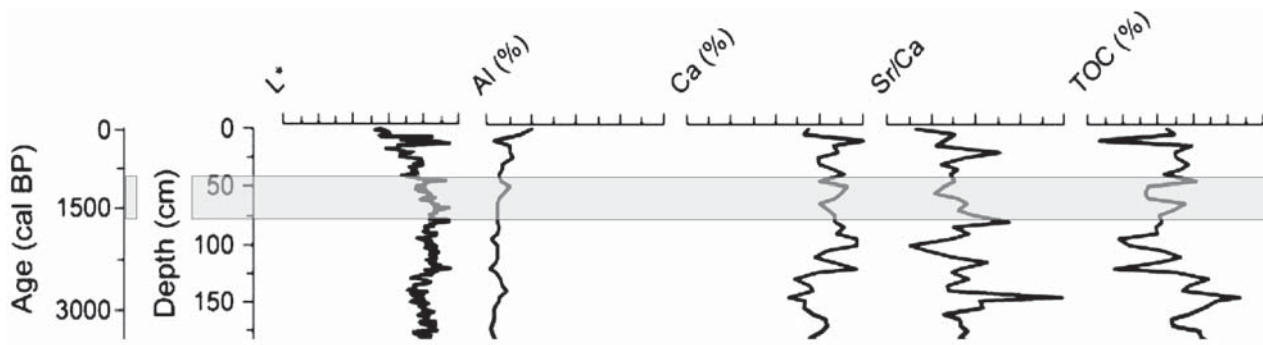


**Fig. 10.** Paleoenvironmental reconstruction of the late Holocene succession of the PP Vrana-2 sediment core, from Lake Vrana, based on geochemical and sedimentological proxies (After: Ilijanić and Miko, 2016, changed by F. Welc).

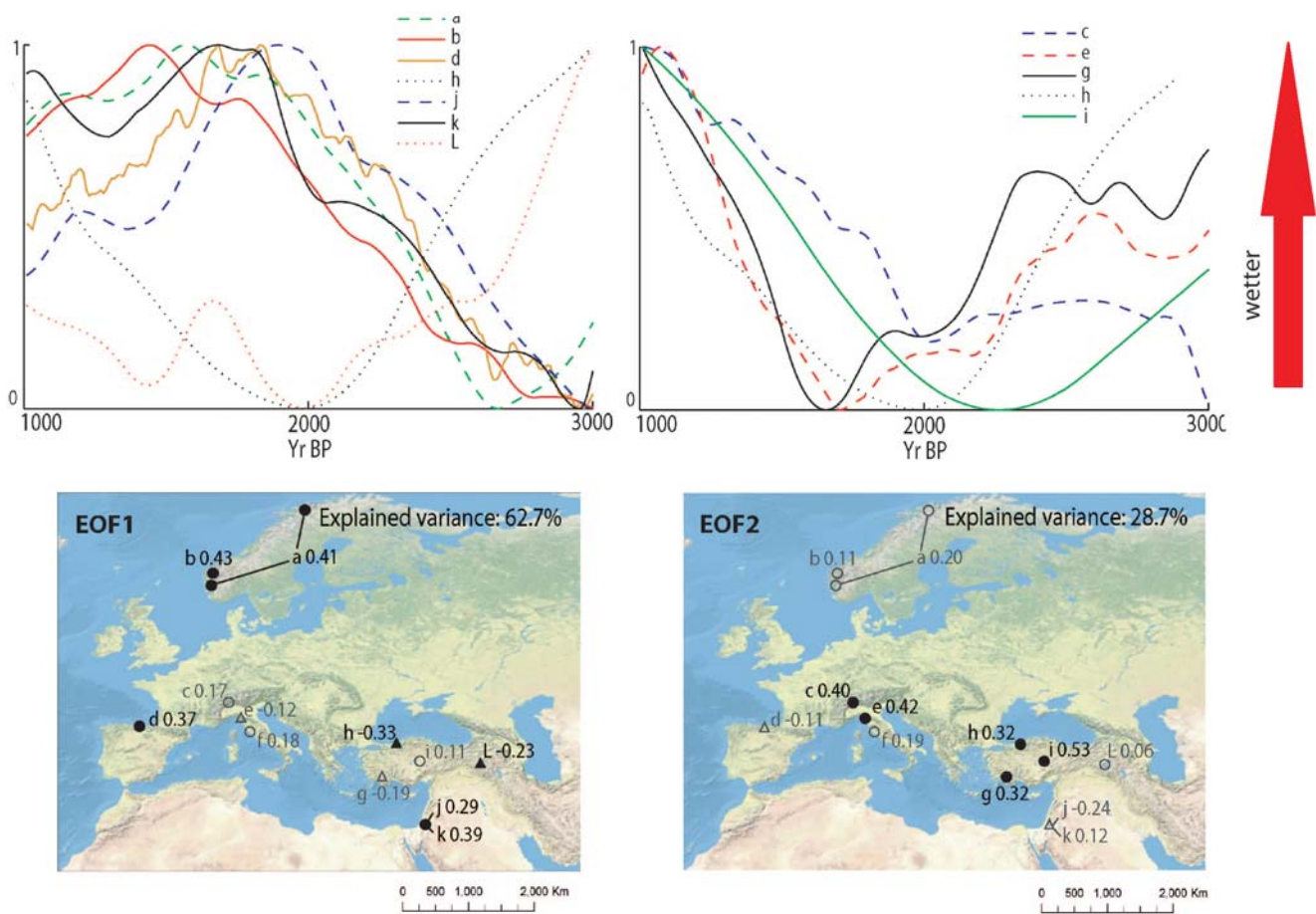


**Fig. 11.** Reconstructed Empirical Orthogonal Function analysis (EOF) of 12 proxy indicators of climatic humidity (see Fig. 12 below). Circles and triangles indicate proxies which are inversely proportional in each mode. Records with the highest loadings are indicated by black symbols whilst records with low values (below the selection threshold) are indicated by hollow symbols. Two carve graphs present scaled 1000 yr running mean of the proxy time series (After: Dermody *et al.*, 2012, changed by F. Welc).

a 1.5 ka BP Bond interval, wetter climatic conditions in Northern Europe coincided with drier conditions in the Mediterranean region (Dermody *et al.*, 2012). To identify the transregional pattern of change in climatic humidity during the Roman Period and after it in the Mediterranean area, Dermody *et al.* (2012) prepared an EOF (Empirical-Orthogonal-Function) analysis model based on a selection

of high quality proxies of climatic humidity (Fig. 10). EOF analysis indicates the dominant pattern of climate variability at 3–1 cal. ka BP. Wet-dry-wet fluctuations in humidity is evident in the Central Mediterranean region and Turkey, whereas a dry-wet-dry fluctuation is indicated in Spain and Israel. The timing of shifts in the seesaw is correlated with 1450 yr cycles in the North Atlantic SST. Based on

ID	Location	Proxy type	Dating uncertainty (years)	Reference
a	Norwegian Coast	Reconstructed glacier dynamics	±50	Bakke <i>et al.</i> (2008)
b	South West Norway	Reconstructed glacier dynamics	±60	Nesje <i>et al.</i> (2000)
c	West Central Alps	Reconstructed glacier dynamics	±200	Holzhauser <i>et al.</i> (2005)
d	Northern Spain	Oxygen isotope ratios in speleothem	±150	Dominguez-Villar <i>et al.</i> (2008)
e	North West Italy	Oxygen isotope ratios in speleothem	±70	Zanchetta <i>et al.</i> (2007)
f	Central Italy	Reconstructed lake levels	±50	Magny <i>et al.</i> (2007)
g	South West Turkey	Stable isotope and pollen	±70	Eastwood <i>et al.</i> (2007)
h	Turkish Black Sea Coast	Uranium isotope ratios in speleothem	±60	Göktürk <i>et al.</i> (2011)
i	Central Turkey	Stable isotope and pollen	±250	Roberts <i>et al.</i> (2001)
j	Dead Sea Israel	Reconstructed lake levels	±50	Bookman <i>et al.</i> (2004)
k	Dead Sea Israel	Reconstructed lake levels	±40	Migowski <i>et al.</i> (2006) Wick <i>et al.</i> (2003) van Zeist and Woldring (1978)
L	South East Turkey	Stable isotope and pollen	±500	Eastwood <i>et al.</i> (2007)

**Fig. 12.** Proxy records of climatic humidity used as input in the empirical orthogonal function (EOF) analysis. The location of the proxy records is illustrated in Fig. 10 (After: Dermody *et al.*, 2012).

EOF analysis, Dermody *et al.* (2012) conclude that climatic humidity oscillations over the Mediterranean during the Roman Period were primarily caused by a modification of the jet stream linked to SST change in the North Atlantic.

Based on the available and still scarce paleoclimatic data, one may conclude that at ca. 1.5 cal. ka BP the lake levels in the Adriatic region were drastically reduced, probably because of strong decrease in humidity. This dry episode can be correlated with the so-called North Atlantic Bond event 3 (Bond *et al.*, 1997). The drought took place at ca. 1.5 cal. ka BP, followed by a humid episode. It seems probable that such sequence of events finds its record in the slope deposits from the archaeological site at Plemići Bay. Full confirmation may be supplied by analysis of analogous deposits in other archaeological sites dated on the Late Antiquity and later in the north-eastern Adriatic region. Moreover, in the future, research at these sites may bring significant palaeoclimatic data crucial for the understanding of transregional climate changes correlated with the 1.5 cal. ka BP event. This becomes a significant issue owing to the fact that, although numerous studies have been devoted to the Holocene terrestrial vegetation history in the central Mediterranean region (Sadori *et al.*, 2011), up to now most lake sediment sequences on which paleoclimatic reconstructions are based are usually poorly dated, or sampled with a resolution not sufficient for the recognition of a detailed sub-millennial late Holocene environmental change (Rudzka *et al.*, 2012).

## CONCLUSIONS

GPR measurements performed close to the remains of the Roman structures at Plemići Bay revealed the outline of a rectangular building ca. 15 m long and at least 5 m wide. The reconstructed plan shows a building that finds

analogies with Roman storehouses (*horreum*), most probably connected with a ceramic production centre operating in the close vicinity. The area occupied by the remains of the Roman pottery workshop was repeatedly covered by immense soil-debris flows, thus silty sand was deposited above the archaeological site and created a slope. Three geological profiles located to the west of the remains of the Roman building were documented using lithological analysis, supplemented by magnetic susceptibility measurements and malacological analysis. The profiles revealed at least three generations of slope sediments. All sedimentary series have been formed in result of intensive soil or debris flows. It can be assumed that the documented layers were transported down slope and deposited on top of the ancient Roman structures during an intensely wet interval. Because they are characterised by a considerable thickness, it can be also supposed that the wet episode was preceded by a relatively long dry interval, during which the plant cover was significantly reduced and extensive erosion processes dominated.

A basic question still remains as to when these large scale slope processes were initiated and when the preceding dry interval occurred. The Roman building covered by the slope series and other ancient structures could be preliminarily dated between the 1<sup>st</sup>–4<sup>th</sup> centuries (Ilkić and Parica, 2017; Lipovac Vrkljan *et al.*, 2017). In all examined profiles, fragments of Roman pottery were found, which suggests that intensification of slope processes took place when the Roman site was already abandoned, thus most probably within the 5<sup>th</sup>–9<sup>th</sup> c. AD. These assumptions seem to confirm paleoclimatic data from the eastern Adriatic region. The lake levels in the region were drastically reduced at ca. 1.5 cal. ka BP, probably because of strong decrease in precipitation. This evident dry episode can be correlated with the so-called North Atlantic Bond event 3. The drought at ca. 1.5 cal. ka BP was followed by a humid episode.

## Acknowledgments

The author would like to thank two anonymous reviewers for their valuable comments and suggestions that have significantly improved the article. Research in the Plemići Bay were realized thanks to the financial support of the project RED – Roman Economy in Dalmatia: production, distribution and demand in the light of pottery workshops (HRZZ, IP-11-2013-3973). Acknowledgments are also addressed to Ana Konestra and Goranka Lipovac Vrkljan (Institute of Archaeology, Zagreb, Croatia) and Kamil Rabięga (Institute of Archaeology, Cardinal Stefan Wyszyński University in Warsaw) for many valuable comments and support during field survey.

## REFERENCES

- Alexandrowicz, S.W., Alexandrowicz, W.P., 2011. Analiza malakologiczna. Metody badań i interpretacji. Rozprawy Wydziału Przyrodniczego PAU 3. Wydawnictwa PAU. Kraków.
- Babić, L., Zupanić, J., 1998. Nearshore deposits in the middle Eocene clastic succession in northern Dalmatia (Dinarides, Croatia). *Geologia Croatica* 51/2, 175–193.
- Bakke, J., Lie, Ø., Dahl, S. O., Nesje, A., Bjune, A. E., 2008. Strength and spatial patterns of the Holocene wintertime westerlies in the NE Atlantic region. *Global and Planetary Change* 60, 28–41.
- Bloemdal, J., deMenocal, P., 1989. Evidence for a change in the periodicity of tropical climate cycles at 2.4 Myr from whole – core magnetic susceptibility measurements. *Nature* 342, 897–900.
- Bond, G., Kromer, B., Beer, J., Muscheler, R., Evans, M. N., Showers, W., Hoffmann, S., Lotti-Bond, R., Hajdas, I., Bonani, G., 2001. Persistent solar influence on North Atlantic climate during the Holocene. *Science* 294, 2130.
- Bond, G., Showers, W., Cheseby, M., Lotti, R., Almasi, P., deMenocal, P., Priore, P., Cullen, H., Hajdas, I., Bonani, G., 1997. A pervasive millennial scale cycle in North Atlantic Holocene and glacial climates. *Science* 278, 1257–1266.
- Bookman, R., Enzel, Y., Agnon, A., Stein, M., 2004. Late Holocene lake levels of the Dead Sea. *Bulletin of the Geological Society of America* 116, 555–571.
- Büntgen, U., Tegel, W., Nicolussi, K., McCormick, M., Frank, D., Trouet, V., Kaplan, J.O., Herzig, F., Heussner, K.U., Wanner, H., Luterbacher, J., Esper, J., 2011. 2500 years of European climate variability and human susceptibility. *Science* 331, 578–82.
- Cech, B., 2017. *Technik in der Antike*, Theiss.
- Conyers, B.L., 2013. *Ground-Penetrating Radar for Archaeology*. 3<sup>rd</sup> Edition. Altamira Press.
- Conyers, B.L., 2016. *Ground-Penetrating Radar for Geoarchaeology*. Wiley and Blackwell.
- Conyers, B.L., 2016a. Ground-Penetrating Radar Mapping Using Multiple Processing and Interpretation Methods. *Remote Sensing* 8, 562, doi:10.3390/rs8070562
- Conyers, B.L., 2018. *Ground-Penetrating Radar and magnetometry for Buried Landscape Analysis*. Springer Briefs in Geography. Springer.
- Conyers, B.L., Leckebusch, J., 2010. Geophysical archaeology research agendas for the future: Some Ground-penetrating Radar examples. *Archaeological Prospection* 17, 117–123.
- Dearing, J.A., 1994. *Environmental magnetic susceptibility: using the Barrington MS2 System*. Chi Publishing. Kenilworth.
- Dermody, B.J., de Boer, H.J., Bierkens, M.F. P., Weber, S.L., Wassen, M.J., Dekker, S.C., 2012. A seesaw in Mediterranean precipitation during the Roman Period linked to millennial-scale changes in the North Atlantic. *Climate of the Past* 8, 637–651.
- Dominguez, S.J., 2011. *Horrea Militaria*. El aprovisionamiento de grano al ejército en el occidente del Imperio romano, *Anejos de Gladius* 14. Madrid.
- Dominguez-Villar, D., Wang, X., Cheng, H., Martin-Chivelet, J., Edwards, R., 2008. A high-resolution late Holocene speleothem record from Kaite Cave, northern Spain:  $\delta^{18}\text{O}$  variability and possible causes. *Quaternary International* 187, 40–51.
- Doom, R., 2009. *The Role of Climate Change in Alluvial Fan Development*, *Geomorphology of Desert Environments*, 2nd edition.
- Dunkeloh, A., Jacobeit, J., 2003. Circulation dynamics of Mediterranean precipitation variability 1948–98. *International Journal of Climatology* 23, 1843–1866.
- Eastwood, W.J., Leng, M.J., Roberts, N., Davis, B., 2007. Holocene climate change in the eastern Mediterranean region: a comparison of stable isotope and pollen data from Lake Gölhisar, southwest Turkey. *Journal of Quaternary Science* 22, 327–341.
- Fritz, F., Pavičić, A., 1991. The Boljkovac spring, Croatia – a case of the overexploitation of a karst spring. XXIII I.A.H. Congress “Aquifer overexploitation”, Proceedings, Canary Islands, Spain, 515–518.
- Giraudi, C., Magny, M., Zanchetta, G., Drysdale, R.N., 2011. The Holocene climatic evolution of Mediterranean Italy: A review of the continental geological data. *The Holocene* 21, 1, 105–115.
- Göktürk, O.M., Fleitmann, D., Badertscher, S., Cheng, H., Edwards, R.L., Leuenberger, M., Fankhauser, A., Tüysüz, O., Kramers, J., 2011. Climate on the southern Black Sea coast during the Holocene: implications from the Sofular Cave record. *Quaternary Science Reviews* 30, 2433–2445.
- Harvey, A., 2002. The Role of Base-Level Change in the Dissection of Alluvial Fans: Case Studies from Southeast Spain and Nevada 45, 67–87.
- Hooke, R., 1967. Processes on Arid-Region Alluvial Fans: *Chicago Journals* 75/4, 438–460.
- Ilijanić, N., Miko, S., 2016. Lake Vrana – Holocene climate archive. In: *Lake – Basin – Evolution Stratigraphy, Geodynamics, Climate and Diversity of Past and Recent Lacustrine Systems*. RCMNS Interim Colloquium 2016 Croatian Geological Society Limnology Workshop 20–24 May 2016, Zagreb, 45–48.
- Ilkić, M., Parica, M., 2017. Podmorski arheološki nalazi u okolici Ljupča. In: Faričić, J. (Ed.), *Ljubač – zrcalo povijesnih i geografskih mijena u sjeverozapadnom dijelu Ravnih Kotara, Sveučilište u Zadru, Župa sv. Martina u Ljupču*. Zadar, 98–111.
- Jones, M.D., Roberts, C.N., Leng, M.J., Turke, M., 2006. A high-resolution late Holocene lake isotope record from Turkey and links to North Atlantic and monsoon climate. *Geology* 34, 361.
- Kacanski, A., Carmi, I., Shemesh, A., Kronfeld, J., Yam, R., Flexer, A., 2001. Late Holocene climatic change in the Balkans: Speleothem isotopic data from Serbia, *Radiocarbon* 43, 647–658.
- Kuzucuoglu, C., Dörfler, W., Kunesch, S.P., Goupille, F., 2011. Mid- to late-Holocene climate change in central Turkey: The Tecer Lake record. *The Holocene* 21/1, 173–188.
- Lipovac Vrkljan, G., Konestra, A., Ilkić, M., Welc, F., Mieszkowski, R., 2017. Project RED’s field activities in 2016: geophysical and filed surveys. *Annales Instituti Archaeologici* 18, 163–166.
- Lipovac Vrkljan, G., Konestra, A., 2018. Approaching the Roman economy of Province Dalmatia through pottery production – the Liburnia case study. In: *Lipovac Vrkljan, Konestra (Eds), Pottery Production, Landscape and Economy of Roman Dalmatia Interdisciplinary approaches*, Archaeopress, Oxford, 14–36.
- Ložek, V., 1964. *Quartärmollusken der Tschechoslowakei*. *Rozpravy Ústředního ústavu geologického* 31, 1-374.
- Magny, M., de Beaulieu, J.-L., Drescher-Schneider, R., Vannięre, B., Walter-Simonnet, A.-V., Miras, Y., Millet, L., Bossuet, G., Peyron, O., Brugiapaglia, E., Leroux, A., 2007. Holocene climate changes in the central Mediterranean as recorded by lakelevel fluctuations at Lake Accesa (Tuscany, Italy). *Quaternary Science Reviews* 26, 1736–1758.
- Majcen, Z., Korolija, B., 1970. Un profil interessant a travers les couches de Ravni Kotari et les iles de Zadar (Ugljan, Iž, Rava, Dugi Otok). *Geoloski Vjesnik* 23, 103–112.

- McCormick, M., Büntgen, U., Cane, M.A., Cook, E.R., Harper, K., Huybers, P., Litt, T., Sturt, Manning, W., Mayewski, P.A., More, A.F.M., Nicolussi, K., Tegel, W., 2012. Climate Change during and after the Roman Empire: Reconstructing the Past from Scientific and Historical Evidence. *Journal of Interdisciplinary History* 43 (2), 169–220.
- Migowski, C., Stein, M., Prasad, S., Negendank, J.F.W., Agnon, A., 2006. Holocene climate variability and cultural evolution in the Near East from the Dead Sea sedimentary record. *Quaternary Research* 66, 421–431.
- Miko, S., Ilijanić, N., Jarić, A., Brenko, T., Hasan, O., Šparica M., Čučuzović, H., Stroj, A., 2015. 2400-year multi-proxy reconstruction of environmental change: the Blue Lake (Modro Jezero, Imotski) sediment record. *Croatian Geological Congress – Osijek 2015*, 177.
- Nesje, A., Lie, Ø., Dahl, S.O., 2000. Is the North Atlantic Oscillation reflected in Scandinavian glacier mass balance records? *Journal of Quaternary Science* 15, 587–601.
- Parica, M., Ilkić, M., 2018. Harbour installations in the context of the pottery workshop in Plemići Bay. In: Lipovac Vrkljan, Konestra (Eds.), *Pottery Production, Landscape and Economy of Roman Dalmatia Interdisciplinary approaches*, Archaeopress, Oxford, 71–75.
- Peck, J.A., King, J.W., Colman, S.M., Kravchinsky, V.A., 1994. A rock magnetic record from lake Baikal, Syberia: Evidence for Late Quaternary climate change. *Earth and Planetary Science Letters* 122, 221–238.
- Petović, S., Gvozdrenović, S., Kica, Z., 2017. An annotated checklist of the marine molluscs of the South Adriatic Sea (Montenegro) and a comparison with those of neighbouring areas. *Turkish Journal of Fisheries and Aquatic Sciences* 17, 921–934.
- Peyron, O., Goring, S., Dormoy, I., Kotthoff, U., Pross, J., de Beaulieu, J.-L., Drescher Schneider, R., Vanniére, B., Magny, M., 2011. Holocene seasonality changes in the central Mediterranean region reconstructed from the pollen sequences of Lake Accessa (Italy) and Tenaghi Philippon (Greece). *The Holocene* 21, 1, 131–146.
- Piva, A., Asioli, A., Trincardi, F., Schneider, R.R., Vigliotti, L., 2008. Late-Holocene climate variability in the Adriatic Sea (Central Mediterranean). *The Holocene* 18, 1, 153–167.
- Rickman, G., 1971. *Roman Granaries and store buildings*. Cambridge.
- Roberts, N., Reed, J.M., Leng, M.J., Kuzucuolu, C., Fontugne, M., Bertaux, J., Woldring, H., Bottema, S., Black, S., Hunt, E., Karabiyikolu, M., 2001. The tempo of Holocene climatic change in the eastern Mediterranean region: new high-resolution craterlake sediment data from central Turkey. *The Holocene* 11, 721–736.
- Rogerson, M., Rohling, E.J., Henderson, G.M., Bujsa, M., Mihevc, A., Prelovšek, M., 2011. Holocene climate oscillations reflected in moisture-source variability in a Slovenian speleothem. Oral presentation on 6th International Conference: Climate Change, The Karst Record, 26–29 June 2011, University of Birmingham.
- Rudzka, D., McDermott, F., Suric, M.A., 2012. Late-Holocene climate record in stalagmites from Modrič Cave (Croatia). *Journal of Quaternary Science* 27 (6), 585–596.
- Sadori, L., Giardini, M., Gliozzi, E., Mazzini, I., Sulpizio, R., Welden A., Zanchetta, G., 2015. Vegetation, climate and environmental history of the last 4500 years at Lake Shkodra (Albania/Montenegro). *The Holocene* 25/3, 435–444.
- Samek, A., 2004. *Atlas muszli ślimaków morskich*. Wydawnictwo Mantis, Olsztyn.
- Sandgren, P., Snowball, I., 2001. Application of mineral magnetic techniques to Paleolimnology. In: Last, W., Smol, J. (Ed.), *Tracking environmental change using lake sediments 2. Physical and geochemical methods*. Kluwer Academic Publishers, Netherlands.
- Schubert, R. J., 1903. Zur Geologie des Kartenblattbereiches Benkovac-Novigrad (29, XIII). III. Das Gebiet zwischen Polešnik, Smilčić and Possedaria. *Verhandlungen Geologischen Reichsanstalt* 14, 278–288.
- Schubert, R.J., 1905. Zur Stratigraphie des istriscilnorddalmatinischen Mitteleocäns. *Jahrbuch Geologischen Reichsanstalt* 55, 153–188.
- Schubert, R.J., Waagen, L., 1913. *Erläuterungen zur Geologischen Karte der Oesterr.-ungar. Monarchie, 1:75.000*. Geologischen Reichsanstalt, Wien, 32.
- Snowball, I.F., 1993. Mineral magnetic properties of Holocene lake sediments and soils from the Karsa Valley, Lappland, Sweden, and their relevance to paleoenvironmental reconstruction. *Terra Nova* 5, 258–270.
- Szymanek, M., 2018. Malacological indicators of the late Antiquity environmental conditions. Case studies of the Plemići (Zadar region) and Podšilo Bay (Island of Rab). In: *The 5<sup>th</sup> Geoarchaeological Conference Late Antiquity and Migration Period in the light of geoarchaeological records from the eastern Mediterranean, eastern Adriatic and adjacent regions*. 23–24<sup>th</sup> October 2018, Book of Abstracts, 2.
- Trzciński, J., Zaremba, M., Rzepka, S., Welc, F., Szczepański, T., 2016. Preliminary report on engineering properties and environmental resistance of ancient mud bricks from Tell el-Retaba archaeological site in the Nile delta. *Studia Quaternaria* 33, 47–56.
- Van Welden, A., Beck, C., Reys, J.L., Bushati, S., Koci, R., Jouanne, F., Mugnier, J.-L., 2008. The last 500 year of sedimentation in Shkodra Lake (Albania/Montenegro): Paleoenvironmental evolution and potential for paleoseismicity studies. *Journal of Paleolimnology* 40, 619–633.
- Van Zeist, W., Woldring, H., 1978. A Postglacial pollen diagram from Lake Van in East Anatolia. *Review of Palaeobotany and Palynology* 26, 249–276.
- Welc, F., 2018. Geoarchaeology of pottery workshop sites in Roman Dalmatia. In: Lipovac Vrkljan, Konestra (Eds.), *Pottery Production, Landscape and Economy of Roman Dalmatia Interdisciplinary approaches*, Archaeopress, Oxford, 62–70.
- Welc, F., Lipovac Vrkljan, G., Konestra, K., Rosić, T., 2017a. Remote sensing of a Roman pottery workshop. Report on a geophysical survey carried out in Crikvenica (ancient Ad Turres, Croatia). *Studia Quaternaria* 34 (2), 119–130.
- Welc, F., Mieszkowski, R., Conyers, L.B., Budziszewski, J., Jedynek, A., 2016. Reading of Ground-Penetrating Radar (GPR) images of Prehistoric flint mine: case study from Krzemionki Opatowskie archaeological site in Central Poland. *Studia Quaternaria* 33 (2), 69–78.
- Welc, F., Mieszkowski, R., Lipovac Vrkljan, G., Konestra, A., 2017. An attempt to integration of different geophysical methods (magnetic, GPR and ERT): A case study from the Late Roman settlement on the Island of Rab (Croatia). *Studia Quaternaria* 34 (2), 47–59.
- Welter-Schultes, F., 2012. *European non-marine molluscs, a guide for species identification*. Planet Poster Editions, Goettingen.
- Wick, L., Lemcke, G., Sturm, M., 2003. Evidence of Lateglacial and Holocene climatic change and human impact in eastern Anatolia: high-resolution pollen, charcoal, isotopic and geochemical records from the laminated sediments of Lake Van, Turkey. *The Holocene* 13, 665–675.
- Zanchetta, G., Drysdale, R. N., Hellstrom, J.C., Fallick, A.E., Isola, I., Gagan, M.K., Pareschi, M.T., 2007. Enhanced rainfall in the Western Mediterranean during deposition of sapropel S1: stalagmite evidence from Corchia cave (Central Italy). *Quaternary Science Reviews* 26, 279–286.
- Zanchetta, G., Sulpizio, R., Roberts, N., Cioni, R., Eastwood, W.J., Siani, G., Caron, B., Paterne, M., Santacrose, R., 2011. Tephrostratigraphy, chronology and climatic events of the Mediterranean basin during the Holocene: An overview. *The Holocene* 21, 1, 33–52.
- Zanchetta, G., Van Welden, A., Baneschi, I., Drysdale, R., Sadori, L., Roberts, N., Giardini, M., Beck, C., Pascucci, V., Sulpizio, R., 2012. Multiproxy record for the last 4500 years from Lake Shkodra (Albania/Montenegro). *Journal of Quaternary Science* 27, 780–789.